

Thermal Rates of Hydrogen Exchange of Methane with Zeolite: A Direct *ab Initio* Dynamics Study on the Importance of Quantum Tunneling Effects

Thanh N. Truong

Department of Chemistry, University of Utah, Salt Lake City, Utah 84112

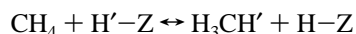
Received: October 21, 1996; In Final Form: February 14, 1997[⊗]

We present a direct *ab initio* dynamics study on the kinetics of the hydrogen exchange of methane with a zeolite model. Dynamical calculations are based on the canonical variational transition state theory plus multidimensional semiclassical tunneling corrections. The reaction path information needed for rate calculations was computed by using a nonlocal hybrid density functional theory with the 6-31G(d,p) basis set. Quantum effects, particularly tunneling, were found to be significant even at the room temperature.

Zeolites are important materials in chemical industry.¹ For instance, in petroleum industry, zeolites have been used as catalysts in cracking, isomerization, and alkylation of hydrocarbons. It has been established that such chemical reactions occur at the zeolite Brønsted acidic sites.^{2–4} However, little is known for certain about the mechanisms of these reactions. Theoretical efforts have been largely limited to electronic structure calculations within the cluster or embedded cluster approach.^{2–4}

Thermal rate constants are essential in modeling zeolite catalytic activity. Furthermore, accurate rate constants are increasingly needed for process simulations. To date, theoretical studies of rate constants for reactions in zeolites are limited to simple transition state theory (TST). Tunneling contribution was treated by the simple Wigner method or simply ignored in many cases.^{5–9} It is known that such a treatment of tunneling significantly underestimates the tunneling probability for proton or hydrogen transfers through moderate barriers. One can expect that for such reactions as hydrogen exchange, dehydrogenation, and hydrogen migration, etc., in zeolites Wigner correction is not adequate, and thus more accurate treatments of tunneling are needed. A direct dynamics approach based on the full canonical variational transition state theory^{10,11} (CVT) plus multidimensional semiclassical tunneling approximations provides a promising solution. Several direct dynamics methodologies^{12–18} for calculating thermal rate constant have been proposed and successfully applied to a wide range of polyatomic gas-phase reactions. In this study, we employed our direct *ab initio* dynamics methodology^{13,14,18–23} for use with density functional theory and/or *ab initio* molecular orbital theory, thus allowing for predictions of thermal rate constants from first principles.

In the present study, we considered the hydrogen exchange reaction of methane with a model of the H-forms of zeolites FAU and MFI,



Thermal rate constants of this reaction were calculated at the CVT level augmented by four different methods for estimating the tunneling contribution. The Wigner method²⁴ assumes that tunneling occurs mostly near the top of the barrier, and thus it requires only the imaginary frequency at the transition state. The Eckart method²⁵ approximates the potential for tunneling by an one-dimensional Eckart function that is fitted to reproduce

the zero-point energy corrected barrier, the enthalpy of reaction at 0 K, and the curvature of the potential curve at the transition state. Both the Wigner and Eckart methods need potential energy information only at the stationary points, and thus they may be used with the TST formalism. The multidimensional semiclassical zero- and small-curvature tunneling methods,²⁶ denoted as ZCT and SCT, respectively, require geometry, energy, gradient, and Hessian information along the minimum energy path (MEP). The ZCT method restricts tunneling path to be along the MEP, whereas the SCT method allows tunneling path to cut corners due to the reaction path curvature. Among these four methods, the SCT approach offers the most accurate treatment of tunneling. Rate calculations were done by using the TheRate (theoretical rate) program²⁷ being developed in our lab.

The potential energy surface information needed for reaction rate calculations was computed directly from the nonlocal hybrid BH&HLYP^{28,29} density functional theory with the 6-31G(d,p) basis set. The BH&HLYP functional has been found to yield more accurate transition state information than the MP2 level³⁰ and other existing DFT functionals. In particular, we found that for similar reactions such as the water-assisted hydrogen atom transfer in formamidine and formamide, the BH&HLYP transition state geometries, frequencies, and barrier heights are closer to the QCISD and CCSD values than the MP2 ones.^{22,31,32} A previous study⁵ showed that with the exception of a small difference on the Mulliken charge of the Al atom, the cluster H₃SiOHAlH₂OSiH₃ as a model of the zeolite active site yields nearly identical transition state structural and energetic information with those from a larger cluster H₃SiOHAl(OH)₂OSiH₃, where hydroxyl groups instead of hydrogens are used to terminate bonds of the aluminum atom. One can then expect no significant difference in the calculated rate between these two zeolite models. In the interest of reducing the computational demand in the rate calculations, we used the smaller cluster in this study.

The optimized transition state structure is shown in Figure 1. No symmetry constraints were used in the optimization, and the normal mode analysis yields only one imaginary frequency of magnitude 1832 *icm*⁻¹ whose eigenvector corresponds to the exchange of the two hydrogen atoms. At the transition state, the BH&HLYP calculated OH and CH bond distances for the transferring H atoms are 1.32 and 1.32 Å, respectively. These can be compared to the results of 1.33 Å for OH and 1.45 Å for CH from the previous Becke–Perdew (BP) calculations⁵ using the DZPV double ζ-basis set plus polarization functions

[⊗] Abstract published in *Advance ACS Abstracts*, March 15, 1997.

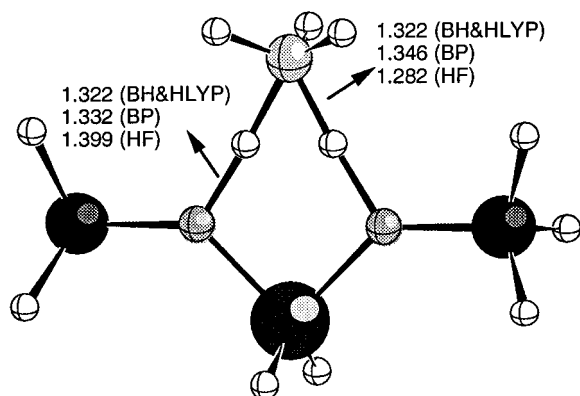


Figure 1. Transition state structure for the hydrogen exchange of methane with the zeolite model. Calculated OH and CH bond distances (Å) are also given (BH&HLYP is from the present study using the 6-31G(d,p) basis set; BP is from ref 5 using the DZPV basis set; HF is from ref 9 using the 6-31G(d,p) basis set).

TABLE 1: Classical and Zero-Point Energy Corrected Barriers, ΔV^\ddagger and ΔV_a^G (kcal/mol), Respectively, for the Hydrogen Exchange of Methane with a Zeolite Model

method/basis	ΔV^\ddagger	ΔV_a^G
BP/DZPV ^a	32.9	29.9
CISD//HF/6-31G(d,p) ^b	36.9	
MP2//HF/6-31++G(d,p) ^c	39.9	37.0
BH&HLYP/6-31G(d,p) ^d	37.7	35.3

^a From ref 5 using the same zeolite model as in this study. ^b From ref 9 using the cluster $\text{H}_3\text{SiOHAl}(\text{OH})_2\text{OSiH}_3$ as a zeolite model. ^c From ref 32 using the cluster HOHAlH_2OH as a zeolite model. ^d This work.

for non-hydrogen atoms and to the previous HF/6-3G(d,p) results⁹ of 1.40 Å for OH and 1.28 Å for CH. The calculated classical and zero-point energy corrected barriers are listed in Table 1 along with previous theoretical data. The BH&HLYP/6-31G(d,p) classical barrier of 37.7 kcal/mol is in accord with the CISD//HF/6-31G(d,p) estimate of 36.9⁹ and MP2//HF/6-31++G(d,p) value of 39.9 kcal/mol.³³ It is noticeably larger than the BP/DZVP barrier by 4.8 kcal/mol. This difference is consistent with our previous results for the hydrogen exchange reaction in the formamidine-water complex.³¹

The focus of this study is on the importance of quantum mechanical tunneling effects in the kinetics of the hydrogen exchange reaction of methane in zeolite. The Arrhenius plot of the calculated thermal rate constants with different tunneling corrections is shown in Figure 2. CVT rate constants per protonic site and transmission coefficients are listed in Table 2. Temperature dependent activation energies are given in Table 3. Due to the substantial barrier, recrossing effects were found to be negligible in the temperature range from 200 to 1000 K; consequently, TST rate constants are nearly identical to the CVT ones. The large curvature in the TST/Eckart, CVT/ZCT, and CVT/SCT Arrhenius curves indicates that quantum tunneling effect is significant. From Figure 2 and Table 2, the present results confirm that the Wigner method significantly underestimates tunneling contribution for temperatures below 600 K. For instance, at the room temperature 300 K, the Wigner method predicts the enhancement factor to the rate constant due to tunneling to be 4.22 while the more accurate SCT method yields a factor of 1210. The large quantum tunneling effect can also be demonstrated by the strong temperature dependence of the activation energy. As seen in Table 3, when using the more accurate tunneling methods, activation energies decrease substantially as the temperature decreases. Our calculated activation energy of 35.4 kcal/mol for the temperature range from 600 to

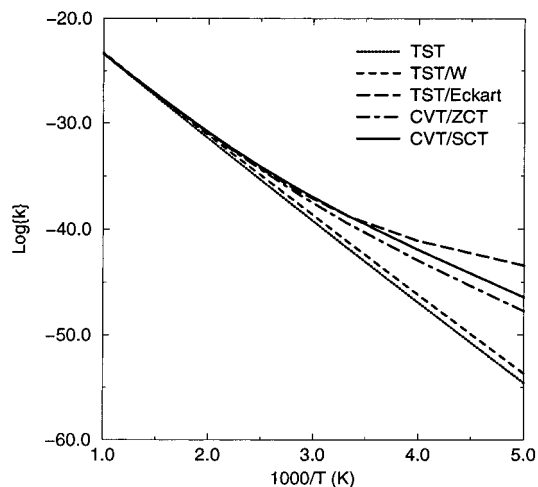


Figure 2. Arrhenius plot of the calculated hydrogen exchange rate constants per protonic site.

TABLE 2: Thermal Rate Constants ($\text{cm}^3 \text{ molecule}^{-1} \text{ s}^{-1}$) and the Transmission Coefficients Using Different Tunneling Methods

T (K)	CVT	transmission coefficients			
		Wigner	Eckart	ZCT	SCT
200	2.63E-55 ^a	8.24	1.44E+11	6.89E+6	1.50E+8
250	1.18E-47	5.63	6.72E+5	9.32E+3	9.38E+4
300	1.53E-42	4.22	1.15E+3	2.27E+2	1.21E+3
400	4.15E-36	2.81	1.19E+1	9.13	1.79E+1
500	3.34E-32	2.16	3.51	3.14	4.17
600	1.47E-29	1.80	2.07	1.93	2.26
800	3.58E-26	1.45	1.27	1.22	1.32
1000	4.61E-24	1.29	1.00	1.02	1.02

^a 2.63E-55 denotes 2.63×10^{-55} .

TABLE 3: Calculated Activation Energies (kcal/mol) for Different Temperature Ranges

T (K)	TST/Wigner	TST/Eckart	CVT/ZCT	CVT/SCT
200-300	34.2	12.8	22.7	21.1
300-600	34.6	28.1	30.0	28.2
600-1000	36.7	35.6	35.7	35.4

1000 K is slightly larger than the experimental data of 29-33 kcal/mol.^{8,34} This is expected because the crystal field (lattice) effects were not included in this study. These effects can be significant as indicated by the large observed variation in the reactivity at different Brønsted acidic sites.⁸ It is possible that the crystal field stabilizes the transition state and further lowers the activation energy. We plan to include such effects in a future dynamical study by using an embedded cluster model. It is interesting to note that even though the Eckart method only uses potential energy information at stationary points, it yields rather accurate tunneling contribution as compared to the SCT results in Table 2. This is consistent with our previous study.²⁵ It is also known that the Eckart method tends to overestimate the tunneling contribution especially at very low temperature. This is because the fitted Eckart function often has a too narrow width. This sometimes compensates for the corner-cutting effect that is not included in the Eckart approach.

The present study illustrates that it is possible with the current computing power to study kinetics and dynamics of reactions in zeolites at a much more accurate level of dynamical theory than the simple TST/Wigner formalism. If computational resources are limited, the present results support the use of the Eckart tunneling method over the Wigner correction. However, with the rapid progress in computer technology, direct dynamics methods such as that used in this study show great promise to

be a routine tool in the field of zeolite chemistry and related areas of oxide catalysis.

Acknowledgment. This work was supported in part by the National Science Foundation via a Young Investigator Award. Computer time provided by the Utah High Performance Computing Center is also gratefully acknowledged.

References and Notes

- (1) *Proceedings from the Ninth International Zeolite Conference*; von Ballmoos, R., Higgins, J. B., Treacy, M. M. J., Eds.; Butterworth-Heinemann: Boston, 1992.
- (2) *Modeling of Structure and Reactivity in Zeolites*; Catlow, C. R. A., Ed.; Academic Press: San Diego, CA 1992.
- (3) Sauer, J. *Chem. Rev.* **1989**, *89*, 199.
- (4) van Santen, R. A.; Kramer, G. J. *Chem. Rev.* **1995**, *95*, 637.
- (5) Blaszkowski, R.; Jansen, A. P. J.; Nascimento, M. A. C.; van Santen, R. A. *J. Phys. Chem.* **1994**, *98*, 12938.
- (6) Blaszkowski, S. R.; van Santen, R. A. *J. Phys. Chem.* **1995**, *99*, 11728.
- (7) Blaszkowski, S. R.; Nascimento, M. A. C.; van Santen, R. A. *J. Phys. Chem.* **1996**, *100*, 3463.
- (8) Kramer, G. J.; van Santen, R. A.; Emeis, C. A.; Nowak, A. K. *Nature* **1993**, *363*, 529.
- (9) Kramer, G. J.; van Santen, R. A. *J. Am. Chem. Soc.* **1995**, *117*, 1766.
- (10) Truhlar, D. G.; Isaacson, A. D.; Garrett, B. C. Generalized transition state theory. In *Theory of Chemical Reaction Dynamics*; Baer, M., Ed.; CRC Press: Boca Raton, FL, 1985; Vol. 4, pp 65–137.
- (11) Tucker, S. C.; Truhlar, D. G. Dynamical formulation of transition state theory: Variational transition states and semiclassical tunneling. In *New Theoretical Concepts for Understanding Organic Reactions*; Bertran, J., Csizmadia, I. G., Eds.; Kluwer: Dordrecht, The Netherlands, 1989; pp 291–346.
- (12) Nguyen, K. A.; Rossi, I.; Truhlar, D. G. *J. Chem. Phys.* **1995**, *103*, 5522.
- (13) Truong, T. N. *J. Chem. Phys.* **1994**, *100*, 8014.
- (14) Truong, T. N.; Duncan, W. T. *J. Chem. Phys.* **1994**, *101*, 7408.
- (15) Truhlar, D. G. Direct dynamics method for the calculation of reaction rates. In *The Reaction Path in Chemistry: Current Approaches and Perspectives*; Heidrich, D., Ed.; Kluwer Academic: Dordrecht, The Netherlands, 1995; pp 229.
- (16) Hu, W.-P.; Liu, Y.-P.; Truhlar, D. G. *J. Chem. Soc., Faraday Trans.* **1994**, *90*, 1715.
- (17) Gonzalez-Lafont, A.; Truong, T. N.; Truhlar, D. G. *J. Phys. Chem.* **1991**, *95*, 4618.
- (18) Truong, T. N.; Duncan, W. T.; Bell, R. L. Direct ab initio dynamics methods for calculating thermal rates of polyatomic reactions. In *Chemical Applications of Density Functional Theory*; Laird, B. B., Ross, R. B., Ziegler, T., Eds.; American Chemical Society: Washington, DC, 1996; Vol 629, pp 85.
- (19) Truong, T. N. *J. Chem. Phys.* **1995**, *102*, 5335.
- (20) Truong, T. N.; Evans, T. J. *J. Phys. Chem.* **1994**, *98*, 9558.
- (21) Duncan, W. T.; Truong, T. N. *J. Chem. Phys.* **1995**, *103*, 9642.
- (22) Bell, R. L.; Taveras, D. L.; Truong, T. N.; Simons, J. *Int. J. Quantum Chem.*, in press.
- (23) Bell, R.; Truong, T. N. *J. Chem. Phys.* **1994**, *101*, 10442.
- (24) Wigner, E. *J. Chem. Phys.* **1937**, *5*, 720.
- (25) Truong, T. N.; Truhlar, D. G. *J. Chem. Phys.* **1990**, *93*, 1761.
- (26) Truhlar, D. G.; Isaacson, A. D.; Skodje, R. T.; Garrett, B. C. *J. Phys. Chem.* **1982**, *86*, 2252.
- (27) Truong, T. N.; Duncan, W. T. *TheRate96, Revision 1.0*; Univeristy of Utah: Salt Lake City, UT, 1996.
- (28) Becke, A. D. *J. Chem. Phys.* **1993**, *98*, 1372.
- (29) Lee, C.; Yang, W.; Parr, R. G. *Phys. Rev. B* **1988**, *37*, 785.
- (30) Möller, C.; Plesset, M. S. *Phys. Rev.* **1934**, *46*, 618.
- (31) Zhang, Q.; Bell, R.; Truong, T. N. *J. Phys. Chem.* **1995**, *99*, 592.
- (32) Bell, R.; Truong, N. T. *J. Chem. Phys.* **1994**, *101*, 10442.
- (33) Evleth, E. M.; Kassab, E.; Sierra, L. R. *J. Phys. Chem.* **1994**, *98*, 1421.
- (34) Larson, J. G.; Hall, W. K. *J. Phys. Chem.* **1965**, *69*, 3080.